

# Predicting the Phase Equilibria of Petroleum Fluids with the SAFT-VR Approach

Lixin Sun, Honggang Zhao, and Clare McCabe

Dept. of Chemical Engineering, Vanderbilt University, Nashville, TN 37235

DOI 10.1002/aic.11110

Published online February 5, 2007 in Wiley InterScience (www.interscience.wiley.com).

*The SAFT-VR equation of state is combined with a semi-continuous thermodynamic approach to model several synthetic and crude oil systems. In our approach, the oil fractions are defined by a continuous distribution that is then represented as discrete pseudo-components using the Gaussian quadrature method. The SAFT-VR parameters for the pseudo-components are obtained from simple linear relationships that were defined in earlier work, which allows the approach to be easily applied to undefined oil systems. Good agreement between the theoretical predictions and experimental data is obtained for bubble point pressure calculations of several gas condensates and the solubility of gases such as methane, ethane, and carbon dioxide in several crude oils. © 2007 American Institute of Chemical Engineers AIChE J, 53: 720–731, 2007*

**Keywords:** equation of state, SAFT-VR, gas condensate, crude oil, solubility, phase equilibria, multicomponent, pseudo-component, mixtures

## Introduction

Enhanced recovery techniques become more attractive and economically feasible as supplies of oil and gas dwindle and become more remote and more challenging to recover, and demand rises, all of which contribute to increasing prices. The challenge of enhanced oil recovery is to release the 40–60% of trapped oil that resists traditional primary and secondary oil production processes. Recovery is typically achieved through the addition of chemicals or heat that will mobilize the gas or oil. The most promising tertiary extraction methods are thermal recovery, chemical recovery, and miscible methods, though alternatives such as microbial enhanced recovery, where oxygen and organic-digesting microbes are injected to digest heavy oil and asphalt allowing a lighter oil to flow, can also be used. In order to optimize these approaches, an understanding of the phase behavior of mixtures containing oil, and enhanced oil recovery fluids, such as carbon dioxide and nitrogen, is essential. Central to achieving this goal is the development of molecular

theories that can accurately predict the phase behavior of multicomponent systems important to enhanced oil recovery processes.

The challenge to modeling the phase equilibrium behavior of oil systems using an equation of state is the complexity of the oil fluid, both in terms of the number of components and the large proportion of undefined components. Typically, the undefined components are identified by a true boiling point distillation analysis and characterized by an average normal boiling point and specific gravity. Such fractions are assumed to contain paraffin, naphthene, and aromatic molecules; however, the chemical nature and concentrations of these molecules are extremely difficult to measure experimentally. As a consequence, a large number of undefined components cannot be characterized; and traditional methods to determine model parameters from pure component data, as is done in a typical equation of state treatment, fail. Therefore, the challenges lie in determining the most appropriate way to group (that is, assign the complex oil fluid a manageable number of pseudo-components) and characterize (that is, determine the parameters of the pseudo-components) these fluids from limited experimental information. Several methods for determining the pseudo-components have been proposed in the literature. Primarily these rely on trial and error, which although

Correspondence concerning this article should be addressed to C. McCabe at c.mccabe@vanderbilt.edu.

time-consuming, can give good results if the procedure to determine the pseudo-components is performed for a sufficiently large number of iterations.

Several groups have proposed specific guidelines for determining the pseudo-components. For example, Lee et al.<sup>1</sup> suggested grouping fractions based on the slopes of available properties (such as density, molecular weight, and so forth) with respect to their boiling points. Li et al.<sup>2</sup> set a fixed number of pseudo-components at every decade range of *K* factors. Pedersen et al.<sup>3</sup> grouped fractions together by assuming that each pseudo-component has an equal weight fraction and its properties are defined through a weight fraction average. The use of such guidelines often results in less calculation time compared to a pure trial-error method; however, such approaches generally lack a rigorous basis. Although complex statistical methods to group pseudo-components have been proposed,<sup>4</sup> they usually require considerable calculations to determine the pseudo-components and do not offer any clear advantage in terms of accuracy over the simpler methods discussed above.

An alternative approach to define oil fractions was proposed by Cotterman et al.<sup>5,6</sup> and used to model polymer and petroleum systems. In their work, the pseudo-components are defined using a continuous distribution in an index property, such as the boiling point, carbon number, or molecular weight. Comparisons of their approach with those using discrete pseudo-components showed significant improvement in both the accuracy and speed of phase equilibria calculations. These findings were further supported by Kehlen et al.<sup>7</sup> in a formal mathematical analysis of continuous thermodynamics. In subsequent work, Cotterman et al.<sup>8</sup> successfully applied this approach to the flash calculation of gas-condensate systems. In the same spirit, Behrens and Sandler<sup>9</sup> proposed a truncated exponential distribution function to model oil mixtures. Furthermore, they demonstrated that discrete pseudo-components can be defined by applying the Gaussian quadrature method to the distribution function. The pseudo-components and their compositions determined at the quadrature points were shown to be mathematically identical to the exponential distribution of the continuous fraction. This approach, therefore, allows the application of semi-continuous thermodynamics in existing codes for multicomponent systems without the need for additional modification. Behrens and Sandler<sup>9</sup> applied their method in combination with the Peng-Robinson equation of state to saturation curve calculations and showed that this approach to semi-continuous thermodynamics not only provides a more rigorous method to choose the pseudo-components, but also gives better results than the more commonly used trial and error techniques. To further improve the semi-continuous thermodynamics method, Willman and Teja<sup>10</sup> subsequently suggested using an effective carbon number (ECN) as a single characterization parameter to differentiate the various isomers of a compound.

When modeling a complex fluid mixture, characterization of the pseudo-components is equally important. Often the chemical makeup of each pseudo-component is divided into three hydrocarbon groups, namely, paraffins (P), naphthenes (N), and aromatics (A), and the composition and properties of the P, N, and A components determined through correlations. This concept has been utilized by numerous researchers, such as Robinson and Peng,<sup>11</sup> Riazi and Daubert,<sup>12,13</sup>

Wang et al.,<sup>14</sup> Huang and Radosz,<sup>15–18</sup> and Shariati et al.,<sup>19,20</sup> to study a range of petroleum fluids. However, since phase equilibrium and thermophysical property calculations are very sensitive to the values of the model parameters in an equation of state, it was suggested by Brule et al.<sup>21</sup> that the conventional correlations used were not suitable for oil system modeling and introduced a potential source of error. For example, the critical properties of extremely heavy oil components are generally unknown, and values obtained by extrapolating critical property correlations developed for smaller molecules are usually inaccurate.<sup>9</sup> In recent years, group contribution methods (critically summarized in Poling et al.<sup>22</sup>) have been used to provide reliable ways to determine properties of heavier molecules based on information about the composition and structure of the pseudo-components; however, the success of such methods depends on the information available on the chemical makeup of the pseudo-components.

In early examples of oil modeling, simple cubic equations of state<sup>3,5,8,9,12,13,23</sup> were widely adopted as modeling tools. However, since the composition and structure of real reservoir fluids can change significantly with time and location, such approaches, which rely on system (composition and state conditions) specific parameters, are not flexible enough to study the changing conditions. Furthermore, cubic equations do not explicitly consider the shape of a molecule and cannot describe association interactions, such as hydrogen bonding, between molecules. The SAFT equation of state, which explicitly takes account of molecular shape, size, and association interactions, has proven to be a very versatile theoretical model<sup>24–27</sup> for describing fluid phase thermodynamics. The SAFT equation, based on Weiertherm's first order thermodynamic perturbation theory for association,<sup>28–33</sup> has been successfully applied to describe the phase behavior of a wide range of industrially important fluids and their mixtures. (For details, the reader is referred to a complete review by Muller and Gubbins.<sup>34</sup>)

In particular, Huang and Radosz<sup>16</sup> applied their engineering version of the SAFT equation to model carbon dioxide and bitumen systems; eight pseudo-components were defined and characterized based on the molecular weight, normal boiling point, and aromaticity of each component, and binary interaction parameters were established as a function of molecular weight and temperature. In more recent work, Ting and co-workers<sup>35</sup> have modeled asphaltene phase equilibrium in a model live (mixture of n-C7 insoluble asphaltenes, toluene, and methane) and a recombined (stock tank oil with its separator gas) oil with the SAFT approach. The recombined oil sample was grouped into six pseudo-components based on composition, the saturate-aromatic-resin-asphaltene fractionation, and gas-oil ratio data, which were characterized by parameters obtained from a direct fit to precipitation data from oil titrations with n-alkanes at ambient conditions.

Of particular relevance to the current work, Buenrostro-Gonzalez et al.<sup>36</sup> investigated asphaltene precipitation in two Mexican crude oils using the SAFT-VR equation, which within the SAFT framework models the dispersion interactions of fluids through potentials of variable attractive range.<sup>37,38</sup> In their work, the parameters for the asphaltene, resin, and oil have a clear physical meaning and can be determined from experimental procedures or calculated

through specific physical relationships or recent theoretical results. For example, the asphaltene monomer parameter was experimentally determined by a fluorescence depolarization technique as described in other work by Buenrostro-Gonzalez.<sup>39</sup> Based on these prior studies, it is evident that the application of the SAFT approach to oil modeling not only provides a theoretical framework with improved predictive power, but also offers an elegant way to consider self-association and cross-association of oil molecules, such as asphaltenes.

In this work we consider the application of the SAFT-VR equation to model the phase equilibria of gas condensates and light petroleum fractions in combination with a semi-continuous thermodynamic approach to describe the oil fluids. The SAFT-VR equation has been successfully applied to describe the thermodynamics and phase behavior of numerous fluids and fluid mixtures, such as n-alkane,<sup>38,40–44</sup> polymers,<sup>45,46</sup> perfluoroalkanes,<sup>47–50</sup> carbon dioxide,<sup>51,52</sup> replacement refrigerants,<sup>53</sup> and electrolytes.<sup>54,55</sup> One important feature of the SAFT-VR equation is that it is possible to develop for a homologous series linear correlations for the model parameters as a function of molecular weight. In previous work,<sup>43</sup> such correlations were successfully established for the alkanes. This feature is of particular importance in our work when defining and characterizing the pseudo-components of undefined oil fractions; if we assume the pseudo-components can be modeled by parameters for the alkanes, we can easily determine the corresponding SAFT-VR parameters from the linear correlations using the molecular weights of each pseudo-component. While this is a simple approach it is not unreasonable, particularly for undefined oil fluids, for which additional fitting would have to be performed in order to determine the PNA fractions. Using this simple approach, good agreement is achieved between the theoretical predictions and experimental data for bubble point pressures and gas solubility in the gas condensates and light oils studied.

The remainder of the article is organized as follows. We begin by outlining the SAFT-VR equation for multicomponent mixtures and the semi-continuous approach used to define the oil fluids. We then present results for the gas condensates and crude oils studied, and comparisons are made with experimental data.

## Models and Theory

The SAFT equation of state for a mixture of associating chain molecules is given in the form of Helmholtz free energy by

$$a(T, \rho, x_i) = a^{IDEAL} + a^{MONO.} + a^{CHAIN} + a^{ASSOC.} \quad (1)$$

where  $a^{IDEAL}$  is the ideal free energy,  $a^{MONO.}$  the excess free energy due to the monomer segments,  $a^{CHAIN}$  the contribution due to the formation of chains from the monomers, and  $a^{ASSOC.}$  the contribution due to intermolecular association. In Eq. 1 all contributions are a function of temperature  $T$ , molar density  $\rho$ , and composition  $\{x_i\}$ . We will consider each contribution in turn for the specific case of the SAFT-VR equation

used in this work; the contribution from association interactions is not discussed as only non-associating molecules are considered in this work.

In the SAFT-VR approach, the monomer dispersion interactions are described through a potential of variable range, in this work a square-well potential

$$u_{ij}(r_{ij}) = \begin{cases} 0 & r_{ij} \geq \lambda_{ij}\sigma_{ij} \\ -\varepsilon_{ij} & \sigma_{ij} \leq r_{ij} < \lambda_{ij}\sigma_{ij} \\ +\infty & r_{ij} < \sigma_{ij} \end{cases} \quad (2)$$

where  $r_{ij}$  is the center-center distance of two monomer segments,  $\sigma_{ij}$  the hard segment diameter, and  $\lambda_{ij}$  and  $\varepsilon_{ij}$  the range and depth, respectively, of the square-well potential between monomer segments  $i$  and  $j$ .

The ideal Helmholtz free energy of a mixture of  $n$  components is given by

$$a^{IDEAL} = \sum_{i=1}^n x_i \ln \rho_i \Lambda_i^3 - 1 \quad (3)$$

where  $\rho_i = N_i/V$  is the molecular number density,  $x_i$  the mole fraction, and  $\Lambda_i$  the thermal de Broglie wavelength of species  $i$ .

The monomer free energy of the mixture is given as

$$a^{MONO.} = \left( \sum_{i=1}^n x_i m_i \right) a^M \quad (4)$$

where  $m_i$  is the number of monomer segments in each chain  $i$ , and  $a^M$  the monomer free energy per segment of the mixture. From the Barker and Henderson high temperature expansion,<sup>56–59</sup> we can obtain the monomer free energy per segment of the mixture as

$$a^M = a^{HS} + a_1/kT + a_2/(kT)^2 + \dots \quad (5)$$

where  $a_1$  and  $a_2$  are the first two perturbation terms associated with the attractive energy  $-\varepsilon_{ij}$ , and in the SAFT-VR approach the series is truncated at second order. The free energy of the reference hard sphere (HS) mixture  $a^{HS}$  is derived from the expression of Boublik<sup>60</sup> and Mansoori et al.<sup>61</sup> as:

$$a^{HS} = \frac{6}{\pi \rho_s} \left[ \left( \frac{\xi_2^3}{\xi_3^2} - \xi_0 \right) \ln(1 - \xi_3) + \frac{3\xi_1 \xi_2}{1 - \xi_3} + \frac{\xi_2^3}{\xi_3(1 - \xi_3)^2} \right] \quad (6)$$

where  $\rho_s = N_s/V = \rho(\sum_{i=1}^n x_i m_i)$  is the number density of spherical segments, and the reduced densities  $\xi_l$  are defined as

$$\xi_l = \frac{\pi}{6} \rho_s \left[ \sum_{i=1}^n x_{s,i} (\sigma_i)^l \right] \quad (l = 1, 2, 3) \quad (7)$$

where  $\xi_3$  is the overall packing fraction of the mixture. In Eq. 7,  $\sigma_i$  is the hard-core diameter of a sphere in chain  $i$  and  $x_{s,i}$  is the mole fraction of spheres of component  $i$  in the mixture, given by

$$x_{s,i} = \frac{m_i x_i}{\sum_{k=1}^n m_k x_k} \quad (8)$$

In the treatment of mixtures, we need appropriate mixing rules to specify the dependence on composition  $x_i$ . In this work we follow the van der Waals (vdW)  $n$ -fluid theories<sup>62,63</sup> in which simple relationships between the pair correlation functions of mixtures and those of pure components are assumed. In the simplest case, for the vdW one-fluid mixing rule, the size, energy, and potential range parameters  $\sigma_x$ ,  $\epsilon_x$ , and  $\lambda_x$  are given by:

$$\sigma_x^3 = \sum_{i=1}^n \sum_{j=1}^n x_{s,i} x_{s,j} \sigma_{ij}^3 \quad (9)$$

$$\epsilon_x = \frac{\sum_{i=1}^n \sum_{j=1}^n x_{s,i} x_{s,j} \epsilon_{ij} \lambda_{ij}^3 \sigma_{ij}^3}{\sum_{i=1}^n \sum_{j=1}^n x_{s,i} x_{s,j} \lambda_{ij}^3 \sigma_{ij}^3} \quad (10)$$

$$\lambda_x^3 = \frac{\sum_{i=1}^n \sum_{j=1}^n x_{s,i} x_{s,j} \epsilon_{ij} \lambda_{ij}^3 \sigma_{ij}^3}{\sum_{i=1}^n \sum_{j=1}^n x_{s,i} x_{s,j} \epsilon_{ij} \sigma_{ij}^3} \quad (11)$$

where variables with subscript  $ij$  refer to the pair interaction between species  $i$  and  $j$ . In order to maintain the accuracy of the description of the structure of the reference fluid, we choose to implement the mixing rule only in the perturbation terms for the monomer interactions, which corresponds to the MIX1b mixing rule of Galindo et al.<sup>37</sup> Hence, the mean-attractive energy  $a_1$  for square-well molecules is given as

$$a_1 = -\frac{2}{3} \rho_s \pi \sum_{i=1}^n \sum_{j=1}^n x_{s,i} x_{s,j} \epsilon_{ij} \sigma_{ij}^3 (\lambda_{ij}^3 - 1) g_0^{HS}[\sigma_x; \zeta_x^{eff}(\lambda_{ij})], \quad (12)$$

and the first fluctuation term in the free energy

$$a_2 = -\frac{1}{2} \rho_s K^{HS} \sum_{i=1}^n \sum_{j=1}^n x_{s,i} x_{s,j} \epsilon_{ij} \alpha_{ij}^{VDW} \times \left\{ g_0^{HS}[\sigma_x; \zeta_x^{eff}(\lambda_{ij})] + \rho_s \frac{\partial g_0^{HS}[\sigma_x; \zeta_x^{eff}(\lambda_{ij})]}{\partial \rho_s} \right\} \quad (13)$$

where  $K^{HS}$  is the isothermal compressibility for a mixture of hard spheres and is given by the Percus-Yevick expression:<sup>64</sup>

$$K^{HS} = \frac{\zeta_0(1 - \zeta_3)^4}{\zeta_0(1 - \zeta_3)^2 + 6\zeta_1\zeta_2(1 - \zeta_3) + 9\zeta_2^3}, \quad (14)$$

The contact value of the radial distribution function,  $g_0^{HS}$ , is given by

$$g_0^{HS}[\sigma_x; \zeta_x^{eff}] = \frac{1 - \zeta_x^{eff}/2}{(1 - \zeta_x^{eff})^3} \quad (15)$$

where the effective packing fraction  $\zeta_x^{eff}$  is given by

$$\zeta_x^{eff}(\zeta_x, \lambda_{ij}) = c_1(\lambda_{ij})\zeta_x + c_2(\lambda_{ij})\zeta_x^2 + c_3(\lambda_{ij})\zeta_x^3 \quad (16)$$

with coefficients

$$\begin{pmatrix} c_1(\lambda_{ij}) \\ c_2(\lambda_{ij}) \\ c_3(\lambda_{ij}) \end{pmatrix} = \begin{pmatrix} 2.25855 & -1.50349 & 0.249434 \\ -0.669270 & 1.40049 & -0.827739 \\ 10.157600 & -15.0427 & 5.30827 \end{pmatrix} \times \begin{pmatrix} 1 \\ \lambda_{ij} \\ \lambda_{ij}^2 \end{pmatrix} \quad (17)$$

The reduced density  $\zeta_x$  in Eq. 16 is defined as

$$\zeta_x = \frac{\pi}{6} \rho_s \sum_{i=1}^n \sum_{j=1}^n x_{s,i} x_{s,j} \sigma_{ij}^3 \quad (18)$$

The contribution to the free energy due to the formation of chain molecules from square-well monomer segments is given by

$$a^{CHAIN} = - \sum_{i=1}^n x_i (m_i - 1) \ln[g_0^{HS}[\sigma_{ii}; \zeta_{ii}^{eff}(\lambda_{ii})] + \beta \epsilon_{ii} g_1^{ii}(\sigma_{ii})]. \quad (19)$$

The term  $g_1^{ii}(\sigma_{ii})$  is obtained from a self-consistent calculation of the pressure using the Clausius virial theorem and the density derivative of the monomer Helmholtz free energy, as described in ref. 38. For a mixture of square-well molecules,  $g_1^{ij}(\sigma_{ij})$  is given by

$$g_1^{ij}(\sigma_{ij}) = \frac{1}{2\pi \epsilon_{ij} \sigma_{ij}^3} \left[ 3 \left( \frac{\partial a_1^{ij}}{\partial \rho_s} \right) - \frac{\lambda_{ij} \partial a_1^{ij}}{\rho_s \partial \lambda_{ij}} \right] = \beta \epsilon_{ij} \left\{ g_0^{HS}[\sigma_x; \zeta_x^{eff}(\lambda_{ij})] + (\lambda_{ij}^3 - 1) \times \frac{\partial g_0^{HS}[\sigma_x; \zeta_x^{eff}(\lambda_{ij})]}{\partial \zeta_x^{eff}} \left( \frac{\lambda_{ij} \partial \zeta_x^{eff}}{3 \partial \lambda_{ij}} - \zeta_x^{eff} \frac{\partial \zeta_x^{eff}}{\partial \zeta_3} \right) \right\} \quad (20)$$

The standard Lorentz-Berthelot combining rules<sup>63</sup> are used to determine the cross, or unlike, parameters in Eqs. 9–20:

$$\sigma_{ij} = \frac{\sigma_{ii} + \sigma_{jj}}{2} \quad (21)$$

$$\epsilon_{ij} = (\epsilon_{ii} \epsilon_{jj})^{1/2} \quad (22)$$

$$\lambda_{ij} = \frac{\lambda_{ii} \sigma_{ii} + \lambda_{jj} \sigma_{jj}}{\sigma_{ii} + \sigma_{jj}} \quad (23)$$

In this work, to represent the oil fractions, a truncated exponential distribution  $F(I)$ , following the procedures outlined by Behrens and Sandler,<sup>9</sup> is used. While Cotterman et al.<sup>5,8</sup> employed a Gaussian distribution function in their work, for most oils an exponential distribution function is sufficient to represent the plot of oil compositions versus carbon numbers.<sup>9</sup> Furthermore, since a finite carbon number must exist

in oil fractions and the distribution cannot continue to infinity, it can be truncated. The truncated distribution is given by:

$$F(I) = e^{-\alpha I} e^{-\beta} \quad (24)$$

where  $A \leq I \leq B$ ,  $A$  is the starting point of the distribution,  $B$  the upper cutoff set at  $C_{50}$  or higher,  $\alpha$  a constant set by the molecular weight of the heavy fraction. The index variable  $I$  is chosen to be a property such as the boiling point, molecular weight, or carbon number, which is used in this work. The parameter  $\beta$  can be found through the normalization condition

$$\int_A^B F(I) dI = x_F \quad (25)$$

where  $x_F$  is the mole fraction of the oil described by the continuous distribution function. Note from Eq. 25,  $e^{-\beta} = \alpha x_F / (e^{-\alpha A} - e^{-\alpha B})$ . In applying the continuous distribution, one frequently needs to compute integrals such as

$$H = \int_A^B f(I) F(I) dI = e^{-\beta} \int_A^B f(I) e^{-\alpha I} dI \quad (26)$$

By transformation of variables

$$H = \int_0^C g(y) e^{-y} dy \quad (27)$$

where

$$y = \alpha(I - A), \quad C = \alpha(B - A) \quad (28)$$

and

$$g(y) = \frac{e^{-\beta} e^{-\alpha A}}{\alpha} f\left(\frac{y}{\alpha} + A\right) \quad (29)$$

Once the Gaussian quadrature method is applied to Eq. 27, the integral can be approximated by

$$H = \int_0^C g(y) e^{-y} dy = \sum_{i=1}^n g(y_i) w_i \quad (30)$$

where  $w_i$  and  $y_i$  are the weights and points, respectively, in the Gaussian quadrature. This means that we can use the discrete pseudo-components in an existing modeling program for multicomponent mixtures, where the pseudo-components are chosen at quadrature points with the mole fractions determined by the weighting at those points. The roots and weights of a two-point (or higher) integration can be generated from a simultaneous set of equations defined by the Gaussian quadrature theory. Behrens and Sandler<sup>9</sup> showed in their work, and it is confirmed in the current work, that usually two or three point integration is sufficient, and four or more components rarely improve the results.

In the implementation of this approach, the parameters of the distribution function (that is,  $A$ ,  $B$ , and  $\alpha$  in Eq. 24) need to be obtained by fitting to the oil fraction to be modeled and the pseudo-components, which correspond to the Gaus-

sian quadrature points, defined. To facilitate explanation, we consider a model oil fraction with mole fraction  $x_f$  and average molecular weight  $M_w$ . We first set the starting carbon number  $N_{c,s}$  to 6 or 7 corresponding to  $C_{6+}$  or  $C_{7+}$  fractions, respectively, and the ending carbon number  $N_{c,e}$  to 50 for most oil systems. We then assume the endpoints of the distribution start and end at the midpoint between these two carbon numbers. Hence, the effective endpoints  $A$  and  $B$  are given by

$$A = N_{c,s} - \frac{1}{2} \quad (31)$$

and

$$B = N_{c,e} + \frac{1}{2} \quad (32)$$

The slope of the distribution,  $\alpha$ , is calculated from the following expression by successive substitutions:

$$\frac{1}{\alpha} = \bar{N}_c - A + \left[ \frac{(B - A)e^{-B\alpha}}{e^{-A\alpha} - e^{-B\alpha}} \right] \quad (33)$$

where the average carbon number  $\bar{N}_c$  is determined from the average molecular weight  $M_w$ . Once the slope is found, the integration range  $C$  is calculated from Eq. 29, and we can generate the roots  $y_i$  and weights  $w_i$  from the Gaussian quadrature theory. Finally, the carbon numbers  $N_{c,i}$  and their mole fractions  $x_i$  of each pseudo-component are determined from the following expressions:

$$N_{c,i} = y_i / \alpha + A \quad (34)$$

and

$$x_i = w_i x_f \quad (35)$$

In the SAFT-VR approach, the model fluid parameters, that is, the hard-core segment diameter,  $\sigma$ , and the range  $\lambda$  and depth of the attractive interaction  $\varepsilon$ , are generally determined from a direct fitting to experimental data. For a homologous series like the  $n$ -alkanes, a simple relationship can be used to determine the number of segments in the model chain from the carbon number:<sup>65</sup>

$$m = 1 + (N_c - 1)/3 \quad (36)$$

and simple linear expressions were developed in earlier work<sup>43</sup> to relate the remaining SAFT-VR parameters to the molecular weight  $M_w$ :

$$m\lambda = 0.039M_w + 0.873 \quad (37)$$

$$m\sigma^3 = 1.566M_w + 24.02 \quad (38)$$

$$m(\varepsilon/k) = 6.343M_w + 76.38 \quad (39)$$

Hence, Eqs. 36–39 provide a method to determine the SAFT-VR parameters for any alkane and a means to easily approximate parameters for other hydrocarbon fluids. Using these relationships, once the carbon number of each pseudo-component ( $N_{c,i}$ ) is known from the semi-continuous thermo-

**Table 1. Compositions of CH<sub>4</sub> & C<sub>6+</sub>, CO<sub>2</sub> & C<sub>6+</sub> Fractions and Specifications of C<sub>6+</sub> Synthetic Oil Components**

	Compositions							
	System 1	System 2	System 3	System 4	System 5	System 6	System 7	System 8
CH <sub>4</sub>	26.75	24.53	24.83	25.44				
CO <sub>2</sub>					25.39	24.96	25.10	25.07
C <sub>6+</sub>	73.25	75.47	75.17	74.56	74.61	75.04	74.90	74.93
<b>C<sub>6+</sub> Specifications</b>								
SG (60/60)	0.704	0.6892	0.7165	0.7203	0.7241	0.7371	0.7537	0.7588
MW	98.81	89.24	115.8	104.63	119.07	146.7	163.96	168.48
Tb (K)	371.33	351.00	403.48	384.06	410.18	454.2	480.2	489.54
<b>Pseudo-Component Specifications</b>								
N <sub>c,1</sub>	6.55	6.17	7.26	6.80	7.42	8.51	9.11	9.28
N <sub>c,2</sub>	11.60	9.40	15.74	13.06	16.71	22.90	26.12	26.95
% of N <sub>c,1</sub>	62.53	64.42	64.15	63.64	63.67	63.52	62.50	62.19
% of N <sub>c,2</sub>	10.72	11.05	11.02	10.92	11.52	11.52	12.40	12.74

dynamic approach described above, we can easily determine the SAFT-VR parameters for each pseudo-component. Therefore, by combining the SAFT-VR equation and semi-continuous thermodynamics, we can easily perform phase equilibrium calculations of an oil fraction as if the system were composed of discrete components of known chemical makeup and composition. We note that our approach does not take into account the ratio of aromatic to saturate components in the oil, which can affect the bubble point, density, and other properties of the oil.

## Results and Discussion

We have applied the SAFT-VR equation together with the semi-continuous thermodynamic approach presented above to study the phase equilibrium of gas condensates and light crude oils. Specifically, we have calculated bubble point pressures of methane and carbon dioxide with synthetic oil or petroleum fractions (C<sub>6+</sub> fractions), and the gas solubility of methane, ethane, and carbon dioxide in crude oil samples (C<sub>7+</sub> fractions).

The synthetic and petroleum oil fractions studied in this work are given in Tables 1 and 2. Table 1 lists the compositions of four methane + synthetic C<sub>6+</sub> mixtures and four carbon dioxide + synthetic C<sub>6+</sub> mixtures,<sup>66,67</sup> while Table 2 gives the compositions of two methane + petroleum C<sub>6+</sub> mixtures and four carbon dioxide + petroleum C<sub>6+</sub> mixtures.<sup>68</sup> Two pseudo-components defined by the quadrature

method described above were used to represent the C<sub>6+</sub> fractions. We note that while the exact compositions are known for the synthetic oil fractions, the compositions of the petroleum fractions are unknown.

In order to demonstrate the effectiveness of the SAFT-VR equation and semi-continuous thermodynamics approach, we have calculated the bubble point pressures of synthetic and petroleum fractions to compare with the experimental data. Results are presented for synthetic oil systems 3 and 5 in Figure 1 and for petroleum oil systems 10 and 14 in Figure 2. As will be noted from Table 1, the C<sub>6+</sub> fractions in system 3 and system 5 have similar molecular weights and boiling temperatures, and therefore the pseudo-components defined are very similar. As seen in Figure 1, the SAFT-VR equation gives a good prediction of the bubble pressure for both system 3 (24.83% C<sub>1</sub> + 75.17% C<sub>6+</sub>) and system 5 (25.39% C<sub>1</sub> + 74.61% C<sub>6+</sub>). Similarly, Figure 2 illustrates that we achieve a good representation of the bubble point pressure for the light petroleum oil system 10 (22.67% C<sub>1</sub> + 77.33% C<sub>6+</sub>) and system 14 (26.27% C<sub>1</sub> + 73.73% C<sub>6+</sub>).

Throughout our work, in order to determine the cross energetic interactions, we used the modified Lorentz-Berthelot rule and introduced a binary interaction coefficient,  $k_{ij}$ , into Eq. 23. We note that this is the only adjustable parameter used in our work; the corresponding parameters for the cross segment diameters and potential widths are not used. The pseudo-components are first defined based on the quadrature method, then characterized by Eqs. 36–39 as described

**Table 2. Compositions of CH<sub>4</sub> & C<sub>6+</sub>, CO<sub>2</sub> & C<sub>6+</sub> Fractions and Specifications of C<sub>6+</sub> Petroleum Components**

	Compositions					
	System 9	System 10	System 11	System 12	System 13	System 14
CH <sub>4</sub>	25.43	22.67				
CO <sub>2</sub>			26.53	24.40	25.19	26.27
C <sub>6+</sub>	74.57	77.33	73.47	75.60	74.81	73.73
<b>C<sub>6+</sub> Specifications</b>						
SG (60/60)	0.7941	0.7640	0.6945	0.7443	0.7941	0.7640
MW	135.17	159.16	101.65	115.66	135.17	159.16
Tb (K)	431.15	473.15	363.15	393.15	431.15	473.15
<b>Pseudo-Component Specifications</b>						
N <sub>c,1</sub>	8.08	8.98	6.67	7.26	8.08	8.98
N <sub>c,2</sub>	20.49	25.42	12.33	15.74	20.49	25.42
% of N <sub>c,1</sub>	63.45	64.79	62.71	64.52	63.65	61.77
% of N <sub>c,2</sub>	11.12	12.54	10.76	11.08	11.15	11.96

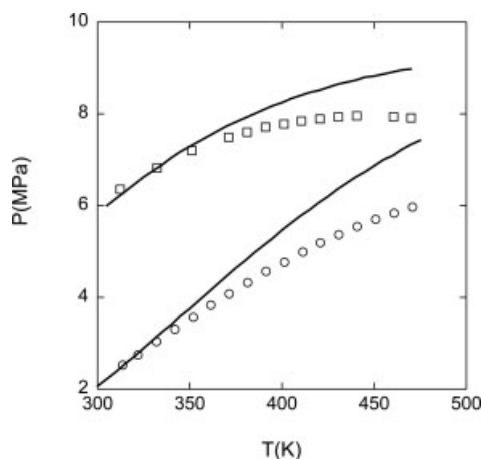


**Figure 1. Bubble point pressures of synthetic oil system 3 (24.83%  $C_1$  + 75.17%  $C_{6+}$ ) and system 5 (25.39%  $CO_2$  + 74.61%  $C_{6+}$ ).**

Solid lines correspond to predictions from the SAFT-VR equation using  $k_{ij} = 0.14$  (system 3) and  $k_{ij} = 0.15$  (system 5); squares correspond to experimental values for system 3<sup>67</sup> and circles for system 5.<sup>66</sup>

above; no other adjustments to the model parameters are performed. For simplicity, we assume a fixed value of  $k_{ij}$  between each pair of components in a given oil mixture and this is determined from a fit to the experimental data. For example, in oil system 10, we assume the value of  $k_{ij}$  between methane and pseudo-component 1, between methane and pseudo-component 2, and between the two pseudo-components are the same, that is,  $k_{ij} = 0.17$ . We note that while this is a somewhat crude assumption, the results are encouraging given the simplicity of the approach, and that the binary interaction parameters obtained are well behaved. For example, we find for a particular oil fluid (that is, for all the  $CH_4$  and  $C_6+$  fractions (systems 1–4) or all the  $CO_2$  and

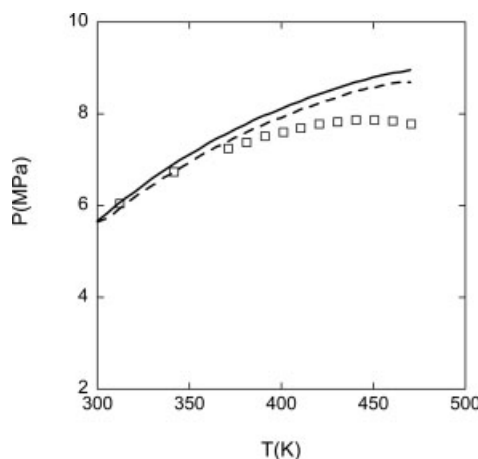


**Figure 3. Bubble point pressures of synthetic oil system 2 (24.53%  $C_1$  + 75.47%  $C_{6+}$ ).**

Solid lines correspond to values predicted from the SAFT-VR equation with two pseudo-components and dashed lines with three pseudo-components, both using  $k_{ij} = 0.13$ . The squares correspond to the experimental data for system 2.<sup>67</sup>

$C_6+$  fractions (systems 5–8) studied) that the binary interaction parameters are very similar and follow a simple linear trend with the oil fraction. We also note that the binary interaction parameters used for the hydrocarbon systems are smaller than those used for the  $CO_2$  systems, which is consistent with earlier work.<sup>69–72</sup> Preliminary calculations indicate that improvement in the prediction of the bubble point pressures at higher temperatures can be obtained if a temperature and/or molecular weight dependent  $k_{ij}$  is used. This will be considered in more detail in future work.

We have also compared the effect of modeling the oil fluid used with two pseudo-components and three pseudo-components. As one can see from Figures 3 and 4, the three pseudo-component representations give slightly better results

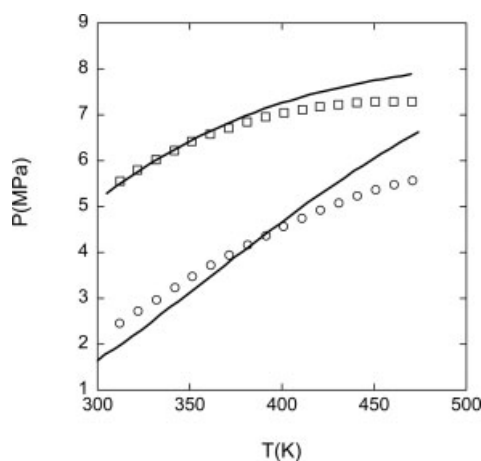


**Figure 2. Bubble point pressures of petroleum oil system 10 (22.67%  $C_1$  + 77.33%  $C_{6+}$ ) and system 14 (26.27%  $CO_2$  + 73.73%  $C_{6+}$ ).**

Solid lines are predictions from the SAFT-VR equation using  $k_{ij} = 0.17$  (system 10) and  $k_{ij} = 0.14$  (system 14); squares are experimental values of system 10 and circles of system 14.<sup>68</sup>

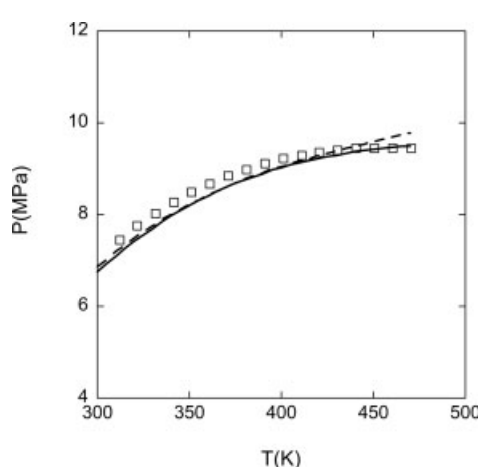


**Figure 4. Bubble point pressures of petroleum oil system 9 (25.43%  $C_1$  + 74.57%  $C_{6+}$ ).**

Solid lines are predictions from the SAFT-VR equation with two pseudo-components and dashed lines from the SAFT-VR equation with three pseudo-components, both using  $k_{ij} = 0.17$ . The squares correspond to the experimental data for system 10.<sup>68</sup>

**Table 3. Comparison of Results Calculated from the SAFT-VR Equation and Experimental Data for Bubble Point Pressure of CH<sub>4</sub> & C<sub>6+</sub> and CO<sub>2</sub> C<sub>6+</sub> Synthetic Oils**

System	Number of Data Points	AAD %		
		This Work	CORGC <sup>a</sup>	PR <sup>b</sup>
1	17	7.00	13.00	3.34
2	13	7.78	8.27	3.32
3	13	10.57	9.86	2.14
4	13	5.11	9.00	2.31
5	17	12.93	3.77	5.72
6	17	9.29	8.01	4.44
7	17	8.41	11.38	2.78
8	17	7.93	10.45	3.90
Overall	124	8.70	9.23	3.58

<sup>a</sup>CORGC with revised group interaction parameters of CO<sub>2</sub> and selected groups for systems 5-8.

<sup>b</sup>Taken from Shariati et al.

over the two pseudo-component description for the synthetic oil system 2 (24.53% C<sub>1</sub> + 75.47% C<sub>6+</sub>), though both overpredict the experimental data at high temperatures. However, the two pseudo-component representation performs well in the higher temperature regions for the light petroleum oil system (system 9) (25.43% C<sub>1</sub> + 74.57% C<sub>6+</sub>).

A comparison between our approach and the chain of rotators group contribution equation of state (CORGC EOS) proposed by Shariati et al.<sup>19</sup> for eight synthetic and seven petroleum oil systems is presented in Tables 3 and 4, respectively. We also include results from the Peng-Robinson (PR) equation, using the characterization algorithm reported by Shariati et al.<sup>19</sup> Overall, the SAFT-VR approach is seen to give better results over the CORGC EOS, except for systems 5, 6, 11, and 12. For the synthetic oil systems, the PR equation is in better agreement with the experimental data than the SAFT-VR or CORGC EOS; however, the SAFT-VR equation is superior for the petroleum oil systems, as shown in Table 3 and 4. For synthetic oil systems, the exact chemical makeup and composition of the model molecules are known, and therefore it is easier to adjust the selection of pseudo-components and achieve good agreement with the experimental data based on the algorithm proposed by Shariati et al.<sup>19</sup> However, for petroleum oil systems, the exact nature and compositions of the oil components are unknown; and as a result, their algorithm does not perform well with either the PR or CORGC equations.

**Table 4. Comparisons of Results Calculated from the SAFT-VR Equation and Experimental Data for Bubble Point Pressure of CH<sub>4</sub> & C<sub>6+</sub> and CO<sub>2</sub> & C<sub>6+</sub> Petroleum Oils**

System	Number of Data Points	AAD %		
		This Work	CORGC <sup>a</sup>	PR <sup>b</sup>
9	17	2.65	12.85	4.92
10	17	4.30	6.82	8.48
11	17	9.53	4.29	7.03
12	17	7.29	2.72	1.45
13	17	7.89	10.41	11.09
14	17	5.45	11.21	1.34
Overall	102	6.18	8.05	5.72

<sup>a</sup>CORGC with revised group interaction parameters for CO<sub>2</sub> and selected groups.

<sup>b</sup>Taken from Shariati et al.

**Table 5. Specifications of Exxon and Jiangsu Crude Oils**

	Oil Mixtures				
	Exxon A Cut 1	Exxon A Cut 5	Exxon B Cut 1	Exxon B Cut 4	Jiangsu
<b>C<sub>7+</sub> Specifications</b>					
SG (60/60)	0.933	1.00	0.944	1.055	n/a
MW (g/mol)	310.7	351.7	282.3	338.5	384.0
Tb (K)	651.2	707.0	630.2	714.0	n/a
<b>Pseudo-Component Specifications</b>					
N <sub>c,1</sub>	13.60	14.61	12.94	14.28	15.48
N <sub>c,2</sub>	38.25	39.83	36.92	39.36	40.87

Finally, we have also applied our SAFT-VR equation with semi-continuous thermodynamics to the calculation of gas solubility in crude oils. Specifically, we have studied the Exxon and Jiangsu crudes reported in the work of Schwarz and Prausnitz<sup>73</sup> and Liu et al.,<sup>74</sup> respectively. The specifications of the Exxon and Jiangsu crude oils (C<sub>7+</sub> fractions) are given in Table 5, along with details of the two pseudo-components used to describe the C<sub>7+</sub> fractions. If we consider the Exxon crudes as representative examples of the accuracy of our approach, we present the solubility of methane in Exxon crude B cut 1 in Figure 5, ethane in Exxon crude A cut 1 in Figure 6, and carbon dioxide in Exxon crude B cut 1 in Figure 7 at various temperatures. As shown by Figures 5–7, the calculations from the SAFT-VR equation are in excellent agreement with the experimental data of Schwarz and Prausnitz.<sup>73</sup>

Overall comparisons between the SAFT-VR approach and the results of Riazi and Vera<sup>75</sup> are given in Table 6. Riazi and Vera adopted both the PNA approach and the single carbon number (SCN) hydrocarbon group approach to investigate the gas solubilities in various petroleum or coal liquid fractions. From the results presented in Table 6, we find that the SAFT-VR equation provides good accuracy in handling the C<sub>7+</sub> crude oil fractions, and performs better than either

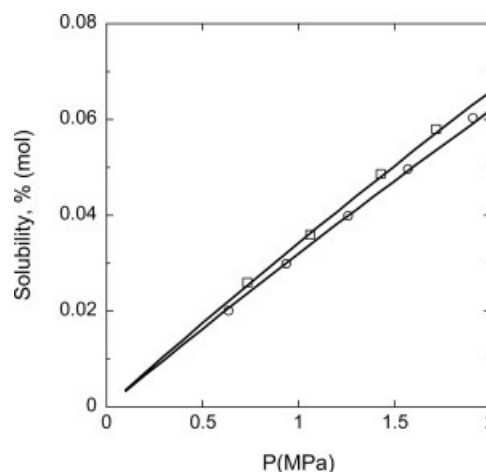


**Figure 5. Solubility of methane in Exxon crude oil B Cut 1.**

Solid lines correspond to predictions from the SAFT-VR equation with  $k_{ij} = 0.05$ ; the squares correspond to experimental data at  $T = 375$  K and the circles experimental data at  $T = 423$  K.<sup>73</sup>



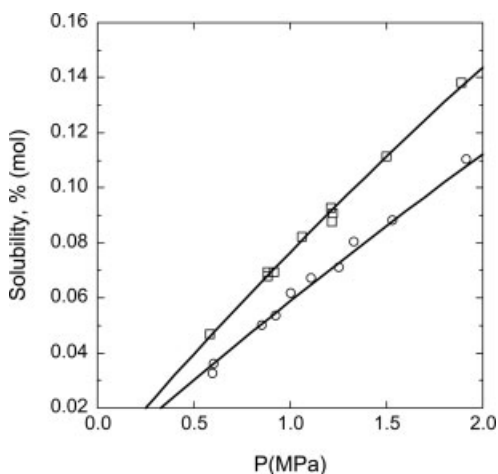


**Figure 6. Solubility of ethane in Exxon crude oil A Cut 1.**

Solid lines correspond to predictions from the SAFT-VR equation with  $k_{ij} = 0.05$ ; the squares correspond to experimental data at  $T = 474$  K and the circles experimental data at  $T = 573$  K.<sup>73</sup>

the PNA or the SCN method by Riazi and Vera.<sup>75</sup> If we consider the Jiangsu crude oils,<sup>74</sup> which represent an even heavier crude oil fraction, the SAFT-VR equation gives an excellent description of the solubility of carbon dioxide in the crude oil for both temperatures (328.15 and 348.15 K) studied and for pressures up to 16 MPa, as shown in Figure 8. Unlike the solubilities of gases in the Exxon crude oils at low pressures, carbon dioxide tends to reach saturation concentrations on a molar basis in the Jiangsu crude oils at higher pressures. As expected, the SAFT-VR equation accurately predicts that the solubility of the gases will increase with pressure and decrease with temperature.

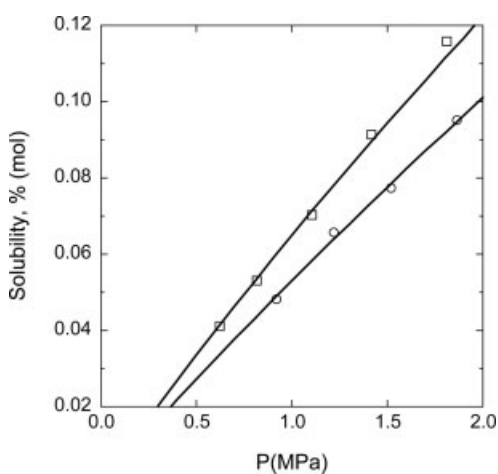


**Figure 7. Solubility of carbon dioxide in Exxon crude oil B Cut 1.**

Solid lines correspond to predictions from the SAFT-VR equation with  $k_{ij} = 0.25$ ; the squares are experimental data at  $T = 375$  K and the circles experimental data at  $T = 425$  K.<sup>73</sup>

**Table 6. Comparison of Results Calculated from the SAFT-VR Equation and Experimental Data for Gas Solubility in Exxon Crude Oils**

Gas	Oil Fraction	T Range (K)	P Range (MPa)	Data Numbers	AAD %		
					This Work	PNA <sup>a</sup>	SCN <sup>a</sup>
CH <sub>4</sub>	Exxon A Cut 1	473–573	0.6–2.1	11	5.10	5.50	5.50
CH <sub>4</sub>	Exxon A Cut 5	473–571	0.8–2.1	10	1.86	4.50	7.50
CH <sub>4</sub>	Exxon B Cut 1	375–423	0.7–2.1	10	1.48	1.40	2.40
CH <sub>4</sub>	Exxon B Cut 4	474–573	0.8–2.1	11	3.50	5.90	4.90
C <sub>2</sub> H <sub>6</sub>	Exxon A Cut 1	473–574	0.6–1.9	20	2.34	5.30	5.30
C <sub>2</sub> H <sub>6</sub>	Exxon A Cut 5	474–574	0.6–2.0	9	1.74	7.30	7.30
C <sub>2</sub> H <sub>6</sub>	Exxon B Cut 1	375–424	0.7–2.0	10	2.59	2.50	3.30
C <sub>2</sub> H <sub>6</sub>	Exxon B Cut 4	474–574	0.7–1.6	11	3.33	2.90	3.10
CO <sub>2</sub>	Exxon A Cut 1	474–571	0.7–1.8	11	1.81	n/a	n/a
CO <sub>2</sub>	Exxon A Cut 5	473–574	0.6–1.8	11	1.99	n/a	n/a
CO <sub>2</sub>	Exxon B Cut 1	374–425	0.6–1.8	10	1.43	n/a	n/a
CO <sub>2</sub>	Exxon B Cut 4	472–571	0.7–1.8	6	3.56	11.00	11.20
Overall				130	2.50	4.89	5.30

<sup>a</sup>PNA and SCN results taken from Riazi and Vera.

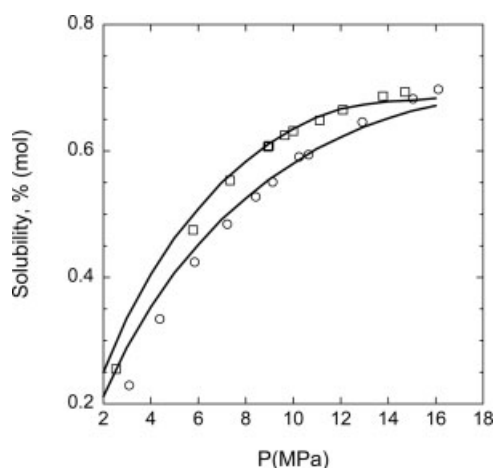


**Figure 8. Solubility of carbon dioxide in Jiangsu crude oil.**

Solid lines correspond to predictions from the SAFT-VR equation with  $k_{ij} = 0.2$ ; the squares are experimental data at  $T = 328.15$  K and the circles experimental data at  $T = 348.15$  K.<sup>74</sup>

## Conclusions

By combining the SAFT-VR equation with semi-continuous thermodynamics, we have successfully applied the SAFT-VR equation to mixtures of gas condensates and crude oils. Good agreement is achieved for phase equilibrium properties when compared to experimental data. While it is recognized that the application of the popular PNA concept can achieve good agreement with experimental data, it usually involves an iterative process to determine the pseudo-components, which is time consuming to develop. Furthermore, the large number of components considered significantly slows down the phase equilibria computation. In contrast, the semi-continuous thermodynamics approach adopted in this work offers a robust method to define the oil fractions and is easy to implement. In addition, the SAFT-VR equation provides a straightforward, yet accurate, method to characterize the defined pseudo-components. The combination of the SAFT-VR equation and the semi-continuous approach enables us to accurately describe not only the bubble point pressures of oil mixtures ( $C_{6+}$  fractions) but also the gas solubilities in crude oils ( $C_{7+}$  fractions).

## Notations

$a$  = Helmholtz free energy; coefficients  
 $c$  = coefficients for effective packing fraction expression  
 $C$  = carbon number  
 $F(I)$  = distribution function of compositions in continuous domain  
 $g$  = radial distribution function  
 $k$  = Boltzmann's constant  
 $K$  = isothermal compressibility  
 $m$  = number of segments in model chain  
 $N$  = number of molecules  
 $p$  = pressure  
 $r$  = distance between molecules  
 $T$  = temperature  
 $u$  = square-well potential  
 $v$  = molar volume  
 $x$  = mole fraction of molecules

## Greek letters

$\varepsilon$  = depth of square-well potential  
 $\Delta$  = difference  
 $\lambda$  = width of square-well potential  
 $\rho$  = density  
 $\sigma$  = hard core diameter  
 $\mu$  = chemical potential  
 $\xi$  = reduced density, packing factor  
 $\Lambda$  = thermal de Broglie wavelength

## Superscripts

ideal = ideal-gas contribution  
mono. = monomer contribution  
assoc. = association contribution  
chain = chain contribution  
eff. = effective  
hs = hard sphere  
i = components

## Subscripts

$c$  = carbon number  
 $ij$  = pair interaction between species  $i$  and  $j$   
 $s$  = segment  
 $x$  = pseudo one-fluid

## Acknowledgments

The authors acknowledge support from the U.S. National Science Foundation under grant number CTS-0452688.

## Literature Cited

1. Lee ST, Jacoby RH, Chen WH, Culham WE. Experimental and theoretical studies on the fluid properties required for simulation of thermal processes. *Soc Petroleum Engineers J.* 1981;21(5):535–550.
2. Li YK, Nghiem LX, Siu A. *Phase Behavior Computation for Reservoir Fluid: Effects of Pseudo Component on Phase Diagrams and Simulation Results.* Presented at 1984 Petroleum Soc. of CIM Annual Technical Meeting, Calgary, June 10–13, 1984.
3. Pedersen KS, Thomassen P, Fredenslund AA. Srk-Eos calculation for crude oils. *Fluid Phase Equilib.* 1983;14(OCT):209–218.
4. Mehra RK. A Statistical Approach for Combining Reservoir Fluids Into Pseudo Components for Compositional Model Studies. Presented at 1982 SPE Annual Technical Conference and Exhibition, New Orleans, Sept. 26–29, 1982.
5. Cotterman RL, Bender R, Prausnitz JM. Phase-equilibria for mixtures containing very many components—development and application of continuous thermodynamics for chemical process design. *Ind Eng Chem Proc Design Development.* 1985;24(1):194–203.
6. Cotterman RL, Dimitrelis D, Prausnitz JM. Supercritical-fluid extraction calculations for high-boiling petroleum fractions using propane—application of continuous thermodynamics. *Berichte Der Deutschen-Gesellschaft-Phys Chem Chem Phys.* 1984;88(9):796–801.
7. Kehlen H, Ratzsch MT, Bergmann J. Continuous thermodynamics of multicomponent systems. *AIChE J.* 1985;31(7):1136–1148.
8. Cotterman RL, Prausnitz JM. Flash calculations for continuous or semicontinuous mixtures using an equation of state. *Ind Eng Chem Proc Design Development.* 1985;24(2):434–443.
9. Behrens RA, Sandler SI. The use of semicontinuous description to model the  $C_{7+}$  fraction in equation of state calculations. *SPE Reservoir Eng.* 1988;August:1041–1047.
10. Willman B, Teja AS. Prediction of dew points of semicontinuous natural-gas and petroleum mixtures. 1. Characterization by use of an effective carbon number and ideal solution predictions. *Ind Eng Chem Res.* 1987;26(5):948–952.
11. Robinson DB, Peng DY. *GPA Research Report.* Tulsa, OK: Gas Processors Association, 1978.
12. Riazi MR, Daubert TE. Prediction of the composition of petroleum fractions. *Ind Eng Chem Proc Design Development.* 1980;19(2):289–294.

13. Riazi MR, Daubert TE. Prediction of molecular-type analysis of petroleum fractions and coal liquids. *Ind Eng Chem Proc Design Development*. 1986;25(4):1009–1015.
14. Wang ZX, Puls JD, Greenkorn RA, Chao KC. Equilibrium vaporization of oils by the chain-of-rotators group contribution equation of state. *Chem Eng J Biochem Eng J*. 1991;46(1):29–34.
15. Huang SH, Radosz M. Phase behavior of reservoir fluids. 2. Supercritical carbon dioxide and bitumen fractions. *Fluid Phase Equilib*. 1990;60:81–98.
16. Huang SH, Radosz M. Phase-behavior of reservoir fluids. 5. Saft model of CO<sub>2</sub> and bitumen systems. *Fluid Phase Equilib*. 1991;70(1):33–54.
17. Huang SH, Radosz M. Phase-behavior of reservoir fluids. 3. Molecular lumping and characterization. *Fluid Phase Equilib*. 1991;66(1–2):1–21.
18. Huang SH, Radosz M. Phase-behavior of reservoir fluids. 4. Molecular-weight distributions for thermodynamic modeling. *Fluid Phase Equilib*. 1991;66(1–2):23–40.
19. Shariati A, Peters CJ, Moshfeghian M. A systematic approach to characterize gas condensates and light petroleum fractions. *Fluid Phase Equilib*. 1999;154:165–179.
20. Shariati A, Peters CJ, Moshfeghian M. Further evaluation of the Shariati-Peters-Moshfeghian C7+ characterization method. *Fluid Phase Equilib*. 2001;179:23–41.
21. Brule MR, Kumar KH, Watanasiri S. Characterization methods improve phase-behavior predictions. *Oil & Gas J*. 1985;83(6):87–93.
22. Poling BE, Prausnitz JM, O'Connell JP. *Properties of Gases and Liquids*. New York:McGraw-Hill Professional; 2000.
23. Peng D-Y, Robinson DB. A new two-constant equation of state. *Ind Eng Chem Fund*. 1976;15(1):59–64.
24. Chapman WG, Gubbins KE, Jackson G, Radosz M. Saft equation-of-state solution model for associating fluids. *Fluid Phase Equilib*. 1989;52:31–38.
25. Chapman WG, Gubbins KE, Jackson G, Radosz M. New reference equation of state for associating liquids. *Ind Eng Chem Res*. 1990;29(8):1709–1721.
26. Huang SH, Radosz M. Equation of state for small, large, polydisperse, and associating molecules. *Ind Eng Chem Res*. 1990;29(11):2284–2294.
27. Huang SH, Radosz M. Equation of state for small, large, polydisperse, and associating molecules—extension to fluid mixtures. *Ind Eng Chem Res*. 1991;30(8):1994–2005.
28. Wertheim MS. Fluids with highly directional attractive forces. 1. Statistical thermodynamics. *J Stat Phys*. 1984;35:19–34.
29. Wertheim MS. Fluids with highly directional attractive forces. 2. Thermodynamics perturbation-theory and integral-equations. *J Stat Phys*. 1984;35:35–47.
30. Wertheim MS. Fluids with highly directional attractive forces. 3. Multiple attraction sites. *J Stat Phys*. 1986;42:459–476.
31. Wertheim MS. Fluids with highly directional attractive forces. 4. Equilibrium polymerization. *J Stat Phys*. 1986;42:477–492.
32. Wertheim MS. Fluids of dimerizing hard-spheres, and fluid mixtures of hard-spheres and dispheres. *J Chem Phys*. 1986;85:2929–2936.
33. Wertheim MS. Thermodynamics perturbation-theory of polymerization. *J Chem Phys*. 1987;87:7323–7331.
34. Muller EA, Gubbins KE. Molecular-based equations of state for associating fluids: a review of SAFT and related approaches. *Ind Eng Chem Res*. 2001;40:2193–2211.
35. Ting PD, Hirasaki GJ, Chapman WG. Modeling of asphaltene phase behavior with the SAFT equation of state. *Petroleum Sci Technol*. 2003;21(3–4):647–661.
36. Buenrostro-Gonzalez E, Lira-Galeana C, Gil-Villegas A, Wu JZ. Asphaltene precipitation in crude oils: theory and experiments. *AIChE J*. 2004;50(10):2552–2570.
37. Galindo A, Davies LA, Gil-Villegas A, Jackson G. The thermodynamics of mixtures and the corresponding mixing rules in the SAFT-VR approach for potentials of variable range. *Mol Phys*. 1998;93(2):241–252.
38. Gil-Villegas A, Galindo A, Whitehead PJ, Mills SJ, Jackson G, Burgess AN. Statistical associating fluid theory for chain molecules with attractive potentials of variable range. *J Chem Phys*. 1997;106(10):4168–4186.
39. Buenrostro-Gonzalez E, Groenzin H, Lira-Galeana C, Mullins OC. The overriding chemical principles that define asphaltenes. *Energy Fuels*. 2001;15(4):972–978.
40. Filipe EJM, de Azevedo E, Martins LFG, et al. Thermodynamics of liquid mixtures of xenon with alkanes: (xenon plus ethane) and (xenon plus propane). *J Phys Chem B*. 2000;104(6):1315–1321.
41. Filipe EJM, Martins LFG, Calado JCG, McCabe C, Jackson G. Thermodynamics of liquid mixtures of xenon with alkanes: (xenon plus n-butane) and (xenon plus isobutane). *J Phys Chem B*. 2000;104(6):1322–1325.
42. McCabe C, Galindo A, Gil-Villegas A, Jackson G. Predicting the high-pressure phase equilibria of binary mixtures of n-alkanes using the SAFT-VR approach. *Int J Thermophys*. 1998;19(6):1511–1522.
43. McCabe C, Jackson G. SAFT-VR modelling of the phase equilibrium of long-chain n-alkanes. *Phys Chem Chem Phys*. 1999;1(9):2057–2064.
44. McCabe C, Galindo A, Cummings PT. Anomalies in the solubility of alkanes in near-critical water. *J Phys Chem B*. 2003;107(44):12307–12314.
45. McCabe C, Galindo A, Garcia-Lisbona MN, Jackson G. Examining the adsorption (vapor-liquid equilibria) of short-chain hydrocarbons in low-density polyethylene with the SAFT-VR approach. *Ind Eng Chem Res*. 2001;40(17):3835–3842.
46. Paricaud P, Galindo A, Jackson G. Recent advances in the use of the SAFT approach in describing electrolytes, interfaces, liquid crystals and polymers. *Fluid Phase Equilib*. 2002;194:87–96.
47. McCabe C, Dias LMB, Jackson G, Filipe EJM. On the liquid mixtures of xenon, alkanes and perfluorinated compounds. *Phys Chem Chem Phys*. 2001;3(14):2852–2855.
48. McCabe C, Galindo A, Gil-Villegas A, Jackson G. Predicting the high-pressure phase equilibria of binary mixtures of perfluoro-n-alkanes plus n-alkanes using the SAFT-VR approach. *J Phys Chem B*. 1998;102(41):8060–8069.
49. Morgado P, McCabe C, Filipe EJM. Modelling the phase behaviour and excess properties of alkane plus perfluoroalkane binary mixtures with the SAFT-VR approach. *Fluid Phase Equilib*. 2005;228:389–393.
50. Bonifacio RP, Filipe EJM, McCabe C, Gomes MFC, Padua AAH. Predicting the solubility of xenon in n-hexane and n-perfluorohexane: a simulation and theoretical study. *Mol Phys*. 2002;100(15):2547–2553.
51. Blas FJ, Galindo A. Study of the high pressure phase behaviour of CO<sub>2</sub>+n-alkane mixtures using the SAFT-VR approach with transferable parameters. *Fluid Phase Equilib*. 2002;194:501–509.
52. Galindo A, Blas FJ. Theoretical examination of the global fluid phase behavior and critical phenomena in carbon dioxide + n-alkane binary mixtures. *J Phys Chem B*. 2002;106(17):4503–4515.
53. Galindo A, Gil-Villegas A, Whitehead PJ, Jackson G, Burgess AN. Prediction of phase equilibria for refrigerant mixtures of difluoromethane (HFC-32), 1,1,1,2-tetrafluoroethane (HFC-134a), and pentafluoroethane (HFC-125a) using SAFT-VR. *J Phys Chem B*. 1998;102(39):7632–7639.
54. Galindo A, Gil-Villegas A, Jackson G, Burgess AN. SAFT-VRE: phase behaviour of electrolyte solutions using the statistical associating fluid theory for potentials of variable range. *J Phys Chem B*. 1999;103(46):10272–10281.
55. Gil-Villegas A, Galindo A, Jackson G. A statistical associating fluid theory for electrolyte solutions (SAFT-VRE). *Mol Phys*. 2001;99(6):531–546.
56. Barker JA, Henderson D. Perturbation theory and equation of state for fluids square-well potential. *J Chem Phys*. 1967;47:2856–2861.
57. Barker JA, Henderson D. Perturbation theory and equation of state for fluids. 2. A successful theory of liquids. *J Chem Phys*. 1967;47:4714–4721.
58. Barker JA, Henderson D. What is liquid – understanding states of matter. *Rev Mod Phys*. 1976;48:587–671.
59. Leonard PJ, Henderson D, Barker JA. Perturbation theory and liquid mixtures. *Trans Faraday Soc*. 1970;66:2439–2452.
60. Boublik T. Hard-sphere equation of state. *J Chem Phys*. 1970;53:471–472.
61. Mansoori GA, Carnahan NF, Starling KE, Leland TW. Equilibrium thermodynamic properties of mixture of hard spheres. *J Chem Phys*. 1971;54:1523–1525.

62. Lee LL. *Molecular Thermodynamic of Nonideal Fluids*. London:Butterworth; 1988.
63. Rowlinson JS, Swinton FL. *Liquid and Liquid Mixtures*. 3rd ed. London:Butterworth Scientific; 1982.
64. Reed TM, Gubbins KE. *Applied Statistical Mechanics*. New York: McGraw Hill; 1973.
65. Archer AL, Amos MD, Jackson G, McLure IA. The theoretical prediction of the critical points of alkanes, perfluoroalkanes, and their mixtures using bonded hard-sphere (BHS) theory. *Int J Thermophys*. 1996;17(1):201–211.
66. Shariati A, Peters CJ, Moshfeghian M. Bubble point pressures of some selected carbon dioxide plus synthetic C6+ mixtures. *J Chem Eng Data*. 1998;43(5):785–788.
67. Shariati A, Peters CJ, Moshfeghian M. Bubble-point pressures of some selected methane plus synthetic C6+ mixtures. *J Chem Eng Data*. 1998;43(2):280–282.
68. Shariati A, Peters CJ, Moshfeghian M. Bubble point pressures of some petroleum fractions in the presence of methane or carbon dioxide. *J Chem Eng Data*. 1998;43(5):789–790.
69. McCabe C, Gil-Villegas A, Jackson G. Predicting the high-pressure phase equilibria of methane plus n-hexane using the SAFT-VR approach. *J Phys Chem B*. 1998;102(21):4183–4188.
70. McCabe C, Jackson G. SAFT-VR modelling of the phase equilibrium of long-chain n- alkanes. *Phys Chem Chem Phys*. 1999;1(9): 2057–2064.
71. McCabe C, Galindo A, Garcia-Lisbona MN, Jackson G. Examining the adsorption (vapor-liquid equilibria) of short- chain hydrocarbons in low-density polyethylene with the SAFT-VR approach. *Ind Eng Chem Res*. 2001;40(17):3835–3842.
72. Galindo A, Blas FJ. Theoretical examination of the global fluid phase behavior and critical phenomena in carbon dioxide plus n-alkane binary mixtures. *J Phys Chem B*. 2002;106(17):4503–4515.
73. Schwarz BJ, Prausnitz JM. Solubilities of methane, ethane, and carbon dioxide in heavy fossil-fuel fractions. *Ind Eng Chem Res*. 1987;26:2360–2366.
74. Liu ZM, Yang GY, Lu Y, Han BX, Yan HK. Phase equilibria of the CO<sub>2</sub>-Jiangsu crude oil system and precipitation of heavy components induced by supercritical CO<sub>2</sub>. *J Supercrit Fluids*. 1999;16(1):27–31.
75. Riazi MR, Vera JH. Method to calculate the solubilities of light gases in petroleum and coal liquid fractions on the basis of their P/ N/A composition. *Ind Eng Chem Res*. 2005;44:186–192.

Manuscript received Mar. 7, 2006, and revision received Sept. 13, 2006, and final revision received Dec. 18, 2006.